

Effect of molecular weight on the cold-crystallization of biodegradable poly(ethylene succinate)

George Z. Papageorgiou, Dimitrios N. Bikiaris, Dimitris S. Achilias*

Laboratory of Organic Chemical Technology, Department of Chemistry, Aristotle University of Thessaloniki, GR-541 24, Thessaloniki, Macedonia, Greece

Received 19 January 2007; received in revised form 28 February 2007; accepted 1 March 2007

Available online 6 March 2007

Abstract

A series of poly(ethylene succinate) (PESu) samples with varying molecular weight were synthesized by the melt polycondensation method. The effect of the molecular weight on the cold-crystallization and the subsequent melting behaviour of melt-quenched PESu was studied by means of standard DSC and Step Scan DSC. Recrystallization and multiple melting followed the cold-crystallization of the samples. In general a melting–recrystallization–remelting scheme was supposed. The phenomenon is more pronounced for the low molecular weight samples. Higher degree of crystallinity is achieved during heating of low molecular weight samples. Cold-crystallization kinetics was also studied using microscopic and macroscopic models. The modified Avrami and the Ozawa methods seem to describe well the experimental data in contrast to the Tobin model. The spherulite growth rates during isothermal crystallization from the melt were studied using polarizing light microscopy (PLM). They were found to decrease with increasing molecular weight. A regime transition was observed at about 70 °C and the K_g^{III}/K_g^{II} ratio was close to 1.8. Furthermore, the nucleation constant K_g of the Lauritzen–Hoffmann equation was estimated using either isothermal PLM measurements or non-isothermal DSC cold-crystallization data and the assumption that the growth rate is inversely proportional to the half crystallization time. No clear trend of K_g with the polymer molecular weight was observed. Finally, the effective activation energy at different relative degrees of crystallinity was estimated using the differential isoconversional method of Friedman. Based on these values, both Lauritzen–Hoffman parameters (U^* and K_g) were evaluated using the overall rates of non-isothermal cold-crystallization according to the method of Vyazovkin and Sbirrazzuoli. A clear increase of U^* with the molecular weight was observed meaning that the effect of diffusion is more pronounced in polymers having higher average molecular weight © 2007 Elsevier B.V. All rights reserved.

Keywords: Poly(ethylene succinate); Biodegradable polymer; Cold-crystallization; Spherulite growth; Isoconversional analysis

1. Introduction

New biodegradable polymers have been developed during last decades in an attempt to face the problem of increasing plastic waste. Aliphatic polyesters have attracted considerable attention due to their combination of biodegradability, biocompatibility and appropriate physical or chemical properties. They are susceptible to microbial attack via enzymatic hydrolysis of their ester groups in their main chains.

Biodegradability of a certain polymer in the form of enzymatic hydrolysis is controlled by several factors. The most important one is the chemical structure of the polymer itself,

meaning the existence of specific chemical bonds along its chain, which might be susceptible to hydrolysis [1,2]. Such groups are those of esters, ethers, amides, etc. It has been reported, that an increase in the polymer average molecular weight up to a critical value leads to decreased biodegradation rates [3–5]. It is also well known that the degree of crystallinity may be a crucial factor, since enzymes mainly attack the amorphous domains of a polymer sample. Copolymers with low crystallinity show increased hydrolysis rates [6,7].

Poly(ethylene succinate) (PESu) is one of the most important, commercially available, synthetic biodegradable polyesters due to its sufficient mechanical properties as well as its high thermal stability [8]. However, only a limited number of works have been published on the crystallization and multiple melting behaviour of this polyester [9–13]. It is well-known that the properties of the final polymeric material are dependent on the morphol-

* Corresponding author. Tel.: +302310 997822; fax: +302310 997769.
E-mail address: axilias@chem.auth.gr (D.S. Achilias).

ogy generated during its processing. Therefore, knowledge of the parameters affecting the crystallization is essential for the optimisation of the processing conditions and the properties of the end product. Research on the polymer crystallization process can be carried out under isothermal or non-isothermal conditions [14]. Analysis of the overall crystallization rate under isothermal conditions is generally accomplished with the use of the so-called Avrami equation [15–19]. However, solidification during polymer processing is always dynamic. Non-isothermal crystallization of polymers is quite difficult to be modelled. Some authors tried to model the non-isothermal process, assuming it can be approximated by a sequence of infinitesimally small isothermal stages, so it can be described based on modifications of the Avrami equation [14].

In a previous paper, synthesis of three polyesters of succinic acid with ethylene, propylene or butylene glycol, by the two-stage melt polycondensation method, was reported [20]. Mathematical modelling of the esterification reaction together with comparative biodegradability studies of the three polyesters, namely, poly(ethylene succinate) (PESu), poly(propylene succinate) (PPSu) and poly(butylene succinate) (PBSu) was presented [21]. It was found that polymer crystallinity plays an important role in the biodegradability of aliphatic polyesters and that PBSu exhibited the lower biodegradation compared to other two polyesters due to its higher crystallinity [21]. Furthermore, in another work, the isothermal crystallization from the melt, as well as the melting behaviour of the isothermally melt-crystallized samples of these three polyesters (PESu, PPSu and PBSu) having the same molecular weight was studied in order to investigate the effect of the variation of the number of the methylene groups in their repeating units on the behaviour of these succinate polyesters [22].

Going a step further, in this work, a detailed study was carried out on the cold-crystallization of quenched PESu samples during heating from the glass, as well as on their subsequent melting behavior. The research was focused on the effect of the molecular weight of PESu. Crystallization kinetics was also analyzed using different macroscopic models in order to test the validity of the equations usually elaborated to describe the process. The effective activation energy was determined using isoconversional approaches. Finally, the Hoffman–Lauritzen parameters (U^* and K_g) were estimated using the overall rates of non-isothermal cold-crystallization according to the method of Vyazovkin and Sbirrazzuoli [23]. Thus, the effect of polymer average molecular weight on both these parameters was evaluated.

2. Experimental

2.1. Materials

Succinic acid (purum 99%), ethylene glycol (purum 99%) and tetrabutoxytitanium used as catalyst (analytical grade) were purchased from Aldrich Chemical Co. Polyphosphoric acid (PPA) used as heat stabilizer was supplied by Fluka. All other materials and solvents used for the analytical methods were of analytical grade.

2.2. Synthesis of poly(ethylene succinate)

Poly(ethylene succinate) (PESu) was prepared by the two-stage melt polycondensation method (esterification and polycondensation) in a glass batch reactor [24]. In short, the proper amount of succinic acid and ethylene glycol in a molar ratio 1/1.1 and the catalyst (10^{-3} mol TBT/mol SA) were charged into the reaction tube of the polyesterification apparatus. The reactor with the reagents was evacuated several times and filled with argon in order to remove the whole oxygen amount. The reaction mixture was heated at 190°C under argon atmosphere and stirring at a constant speed (500 rpm). This first step (esterification) is considered to be complete after the collection of theoretical amount of H_2O , which was removed from the reaction mixture by distillation and collected in a graduate cylinder.

In the second step of polycondensation, PPA was added (5×10^{-4} mol PPA/mol SA), in order to prevent side reactions such as etherification and thermal decomposition. A vacuum (5.0 Pa) was applied slowly over a period of about 30 min, to avoid excessive foaming and to minimize oligomer sublimation, which is a potential problem during the melt polycondensation. In order to prepare samples with different molecular weight, polycondensation was performed at different temperatures such as 170, 200, 220, 230 and 250°C . Polycondensation time was constant at 60 min, for all prepared polyesters while stirring speed was increased at 720 rpm. After the completion of the polycondensation reaction, the polyesters were easily removed, milled and washed with methanol. Detailed presentation of the synthesis of the samples can be found in a previous paper [25].

2.3. Measurements

2.3.1. Intrinsic viscosity

Intrinsic viscosity $[\eta]$ measurements were performed, by using an Ubbelohde viscometer at 25°C . All polyesters were dissolved in chloroform at room temperature in order to prepare solutions with concentrations up to 1 wt% and filtered through a disposable membrane filter $0.2\ \mu\text{m}$ (Teflon). Intrinsic viscosity (IV) was calculated after the Solomon–Ciuta equation: [26]

$$[\eta] = \left\{ 2 \left[\frac{t}{t_0} - \ln \left(\frac{t}{t_0} \right) - 1 \right] \right\}^{1/2} C^{-1} \quad (1)$$

where c is the concentration of the solution; t , is the flow time of solution and t_0 the flow time of pure solvent.

2.3.2. Gel permeation chromatography (GPC)

GPC analysis was performed using a Waters 150C GPC equipped with differential refractometer as detector and three ultrastayragel (10^3 , 10^4 , 10^5 Å) columns in series. CHCl_3 was used as the eluent (1 mL/min) and the measurements were performed at 35°C . Calibration was performed using polystyrene standards with a narrow molecular weight distribution.

2.3.3. Carboxyl end-group content

Carboxyl end-group content (–COOH) of the resins was determined as follows: About 0.1 g of polyesters was dissolved in chloroform at room temperature and the solution was titrated by using a standard NaOH in methanol (N/10) and phenol red as indicator.

2.3.4. Nuclear magnetic resonance (NMR)

¹H-NMR spectra of polyesters were obtained with a Bruker AMX 300 spectrometer operating at a frequency of 300 MHz for protons. Deuterated chloroform (CDCl₃) was used as solvent in order to prepare solutions of 5% w/v. The number of scans was 10 and the sweep width was 6 kHz.

2.4. Differential scanning calorimetry (DSC)

Non-isothermal crystallizations were performed in a Perkin–Elmer Pyris 1 differential scanning calorimeter. A Perkin–Elmer Intracooler IIP was connected to the DSC to achieve high cooling rates. The instrument was calibrated with high purity indium and zinc standards. It is important for the crystallization experiments to minimize the thermal lag, so low-mass samples of about 5 mg were used. For non-isothermal crystallizations, the samples were first melted to 130 °C for 3 min and then rapidly cooled to –50 °C by 500 °C/min. It should be noted here that PESu samples do not crystallize during cooling if a rate faster than 10 °C/min is applied. Subsequently, heating scans at rates 2.5, 5, 7.5, 10, 15 and 20 °C/min were performed in the range from –50 to 130 °C. Kinetic analysis was based on integration of the first, low temperature cold-crystallization exothermic peak, observed on heating of the quenched samples, after subtraction of the corresponding baseline at the same heating rate in the temperature range of interest. To evaluate the samples' ultimate degree of crystallinity, the heat of fusion calculated from integration of the melting peaks was used together with the enthalpy of fusion of the pure crystalline PESu, estimated in [22].

Modulated Temperature DSC experiments were also carried out using the same Pyris 1 DSC and the Perkin Elmer Step Scan software. Step-Scan DSC is a temperature modulated DSC technique. The approach applies a series of short interval heating and isothermal steps to cover the temperature range of interest. With this TMDSC approach, two signals are obtained. Apparent thermodynamic C_p signal represents the reversible aspects of the material, while the isothermal signal reflects the irreversible nature of the sample during heating. For the heating scans in this work a program involving short heating steps of 2.5 °C at a rate 5 °C/min, between true isothermal steps of 0.5 min was applied in the temperature from –35 to 135 °C. The average heating rate was 2.5 °C/min.

2.5. Polarizing light microscopy (PLM)

Measurement of the radius growth rate of PESu spherulites under isothermal crystallisation was investigated using a polarizing optical microscope (Nikon, Optiphot-2) equipped with a Linkam THMS 600 heating stage, a Linkam TP 91 control unit

and also a Jenoptic ProgRes C10plus camera with the Capture Pro 2.1 software. By plotting spherulite radius versus time at different crystallization temperatures, the spherulitic growth rate, *G* can be estimated from the slope of the straight lines obtained.

3. Results and discussion

3.1. Synthesis and characterization of the samples

As it was described in the experimental section, synthesis of PESu samples was performed following the two-step melt polycondensation method. In the first stage of the polymerisation process, succinic acid reacts with ethylene glycol at an elevated temperature (190 °C), forming oligomers, while water is removed from the reactor as by-product. In order to prepare polyesters with different average molecular weights, the second step, involving polycondensation of oligomers, was performed at a series of temperatures ranging between 170 and 250 °C [21]. Results on the characterization of the synthesized PESu samples are shown in Table 1. As one can see, the average molecular weight values of the samples were quite different covering a wide range. At low temperatures, the removal of water and ethylene glycol (formed as by-products) from the melt is difficult and as a result polycondensation proceeds with very low rate. At high temperatures (230–250 °C) polymers with higher molecular weight are prepared, the optimum value being achieved at 250 °C. This value however, cannot be exceeded due to the initiation of thermal degradation [25]. In the following text, the prepared samples are coded using their intrinsic viscosity values. It was preferred to use the IV instead of the corresponding number average molecular weight since there results are more reliable

The appearance of the samples varied with molecular weight. The samples with low molecular weight (PESu 0.15 and 0.28) were rather brittle, while those with higher molecular weight (PESu 0.57 and 0.69) were more tough with tensile strength at break higher than 28 MPa and elongation at break >500%. The number of carboxyl end groups gradually decreased from oligomers till intrinsic viscosity 0.57 dL/g. A small increase in IV and a light brown colour observed for the PESu 0.69 is possibly an indication of degradation reactions at high reaction temperature (250 °C). From DSC thermograms, it was found that the melting temperatures of the polyesters shifted to higher values as the molecular weight increased, while the heat of fusion was reduced (Table 1). Furthermore, the ¹H-NMR spectrum of PESu was very simple, containing only two characteristic peaks at 2.55–2.67 and 4.18–4.3 ppm attributed to methylene proton *a* of succinic acid and *b* of ethylene glycol, respectively.

3.2. Cold-crystallization and melting behavior of PESu

PESu shows slow crystallization on cooling from the melt. It does not crystallize if it is cooled by 10 °C/min or faster. Subsequent heating scans however after rapid cooling from the melt, give cold-crystallization of the polymer. For the study of the cold-crystallization and the melting of non-isothermally cold-crystallized PESu, all of the five PESu polymers with different

Table 1
 Intrinsic viscosity, IV, number average molecular weight, \bar{M}_n , weight average molecular weight, \bar{M}_w , polydispersity, \bar{M}_w/\bar{M}_n , melting temperature, T_m , heat of fusion, ΔH_m and carboxyl number, $[-\text{COOH}]$, of PESu samples prepared at different polycondensation temperatures, T_{pol}

T_{pol} (°C)	IV (dL/g)	\bar{M}_n	\bar{M}_w	\bar{M}_w/\bar{M}_n	T_m (°C)	ΔH_m (J/g)	$[-\text{COOH}]$ (equiv/ 10^{-6})
170	0.15	3560	9820	2.76	101	67.7	178
200	0.28	6810	17980	2.64	102	67.7	80
220	0.41	11350	29050	2.56	103	61.0	39
230	0.57	17100	43780	2.56	105	59.1	16
250	0.69	21480	53700	2.5	106	54.2	21

molecular weight values were tested. Fig. 1 shows the normalized DSC heating scans from the glass for the PESu samples. As one can see the cold-crystallization involves two stages. The first stage is supposed to be associated with the growth of spherulites, which were nucleated on cooling from the melt. PLM observations showed slow nucleation rates for PESu [22]. A second exothermic event occurring at much higher temperature, is most probably associated with recrystallization after partial melting of the unstable crystallites. Cold-crystallization is expected to result in generation of poor crystals and a significant portion of rigid amorphous phase. After partial melting of the poor crystals and relaxation of the rigid amorphous phase the respective fractions of the material might participate in the subsequent

recrystallization [27]. DSC traces of Fig. 1 show clearly the effect of the heating rate.

For each polymer sample, increase of the peak temperature, corresponding to the first cold-crystallization and peak broadening was observed with increasing heating rate. The recrystallization peak temperature depends on the molecular weight of the polymer, but it is always higher than 70 °C. Comparing to the main cold-crystallization peak, it was much less affected by the increase of heating rate and slightly shifted to higher temperatures. In advance, two melting peaks were recorded. This phenomenon was more pronounced for low molecular weight samples, which also exhibited larger recrystallization peaks at a given heating rate. In fact, melting is also

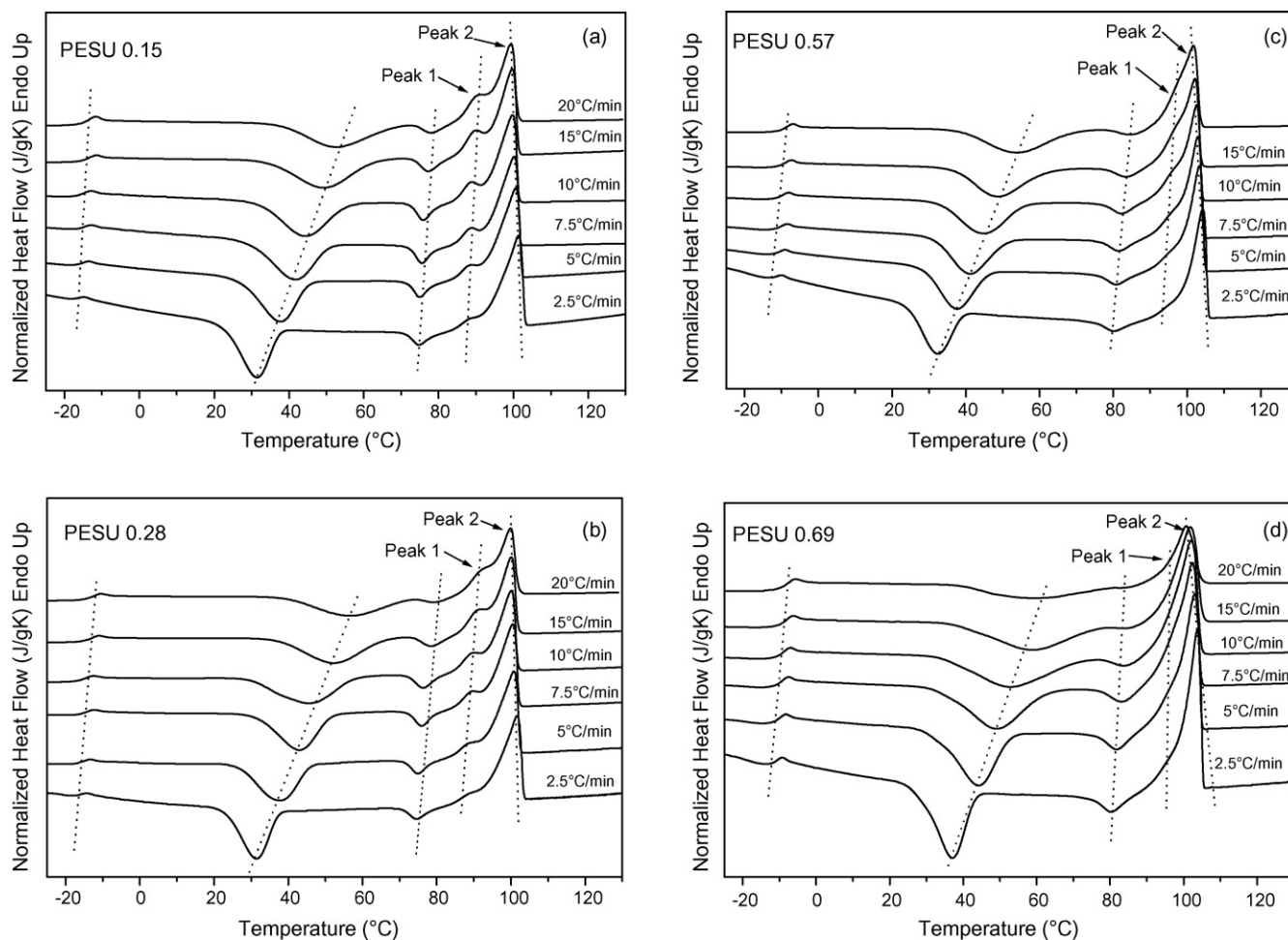


Fig. 1. DSC curves of PESu samples on heating by different scanning rates. (a) PESu 0.15; (b) PESu 0.28; (c) PESu 0.57; and (d) PESu 0.69.

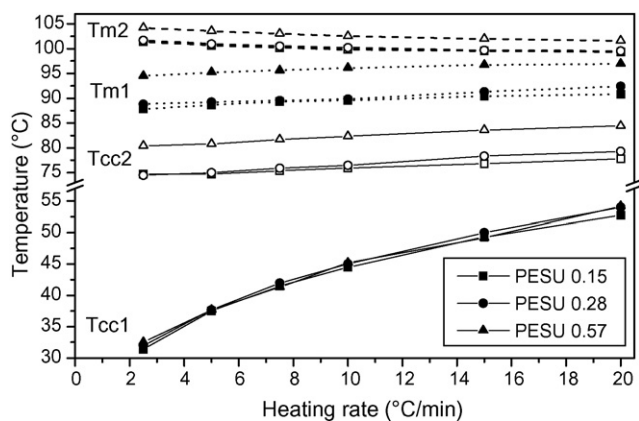


Fig. 2. Variation of the peak temperature of cold-crystallization 1 (T_{cc1}), recrystallization (T_{cc2}), melting peak 1 (T_{m1}) and ultimate melting (T_{m2}). Squares are for PESu 0.15, Circles for PESu 0.28 and up triangles for PESu 0.57.

expected to occur before recrystallization. However, only two of the melting peaks are observable in the standard DSC heating traces, from which the one observed at lower temperature (peak 1) increases in temperature and heat of fusion with increasing heating rate. On the other hand, the ultimate peak (peak 2) for

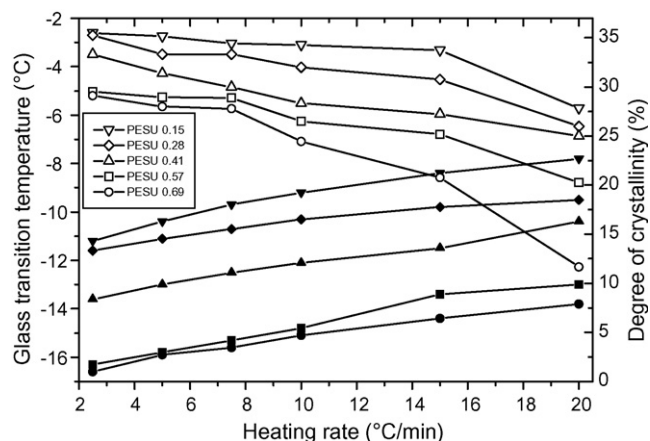


Fig. 3. Dependence of the glass transition temperature and degree of crystallinity after cold-crystallization of the PESu samples on the heating rate. Solid symbols correspond to T_g values, and open symbols to the degree of crystallinity.

all samples decreases with heating rate in both peak temperature and heat of fusion.

At high heating rate scans the recrystallization is prevented or restricted due to less available time. Overall, the picture

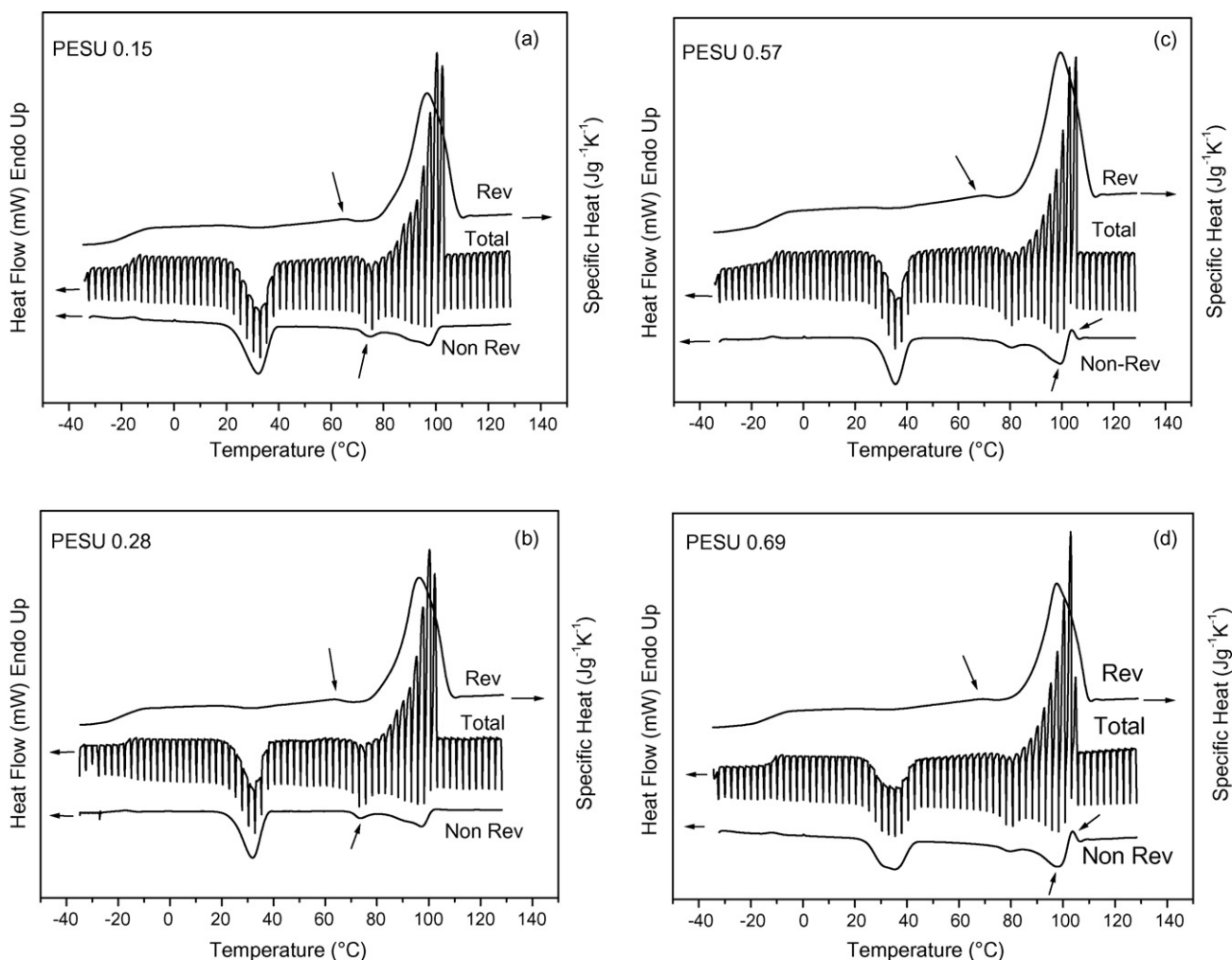


Fig. 4. Step scan TMDSC curves showing reversing, total and non reversing events, for the PESu samples with different molecular weights: (a) PESu 0.15; (b) PESu 0.28; (c) PESu 0.57; (d) PESu 0.69. Arrows indicate the events discussed in the text.

seems to be consistent with the melting–recrystallization–final melting scheme proposed for multiple melting of polymers [28–33]. After cold-crystallization and for high molecular weight samples, the range where (observable) melting occurred was narrower, and the respective peaks were sharper with higher peak temperature (Fig. 2), indicating a more uniform distribution of crystals with respect to crystal size and stability. In contrast, the final degree of crystallinity at a given heating rate was always higher for the low molecular weight samples, mainly due to the effect of chain entanglements. As one can see in Fig. 3 for given molecular weight the crystallinity decreased with increasing heating rate, since the available time for crystallization was reduced.

Fig. 3 also shows the dependence of the glass transition temperature (T_g) on the molecular weight and heating rate. T_g values, at a given heating rate, increased with molecular weight due to reduction in chain mobility. For a certain molecular weight, T_g increased with heating rate. This is related with the relaxation times involved in glass transition. In tune with the observations for T_g , the first cold-crystallization peak temperature, at a given heating rate, is increased with the molecular weight while, for given temperature, the cold-crystallization was slower. At a specific heating rate, the phenomenon for higher molecular weight samples takes place at higher temperatures, but then the available time before approximating the melting region is less, and this in turn results in reduced crystallinity.

Thermal behavior of the glassy PESu samples was also studied by means of Step Scan DSC. For all the samples, in the reversible signal curve a small broad endothermic peak, associated with melting of poor crystals, was observed in the temperature range between the two exothermic events observed in the respective non-reversible signal curve (Fig. 4). Also, one single melting peak was observed at higher temperatures in the reversible signal curve, in contrast to standard DSC thermograms or the total heat flow of TMDSC curves which showed double peaks. From the non-reversing signal curves it was also concluded that the recrystallization occurred in the range from approximately 15 °C above the end of the first cold-crystallization peak up to the end of melting. For samples of lower average molecular weight a significant portion of exothermic events appeared at lower temperatures (Fig. 4). For higher molecular weight PESu, recrystallization occurs mainly close to the final melting and also there is some non-reversing melting observable, proving the stability of the original crystals in this case. After, all it is clear that there is a continuous melting–recrystallization–remelting process and the total heat flow shows only the net effect of exothermic and endothermic phenomena.

3.3. Cold-crystallization kinetics

Initially, it should be clear that from the two exothermic events recorded during the DSC heating scans of the quenched PESu samples (i.e. cold-crystallization and recrystallization), kinetics involved in the first process, are analyzed in the following.

To study the effect of the molecular weight on the cold-crystallization kinetics of PESu, four samples were selected namely PESu-0.15, PESu-0.28, PESu-0.41 and PESu-0.57, corresponding to number average molecular weights, 3560, 6810, 11350 and 17100, respectively. Usually in literature non-isothermal crystallization during cooling is studied and several models have been developed. However, it is believed that the non-isothermal crystallization kinetics during heating (i.e. cold-crystallization) can be described using the same models.

From the dynamic crystallization experiments, data for the crystallization exotherms as a function of temperature dH_c/dT can be obtained for each cooling or heating rate. Then, the relative crystallinity as a function of temperature $X(T)$ can be calculated as follows:

$$X(T) = \frac{\int_{T_0}^{T_c} (dH_c/dT)dT}{\int_{T_0}^{T_\infty} (dH_c/dT)dT} \quad (2)$$

where T_0 denotes the initial crystallization temperature and T_c , T_∞ the crystallization temperature at time t and after the completion of the crystallization process, respectively.

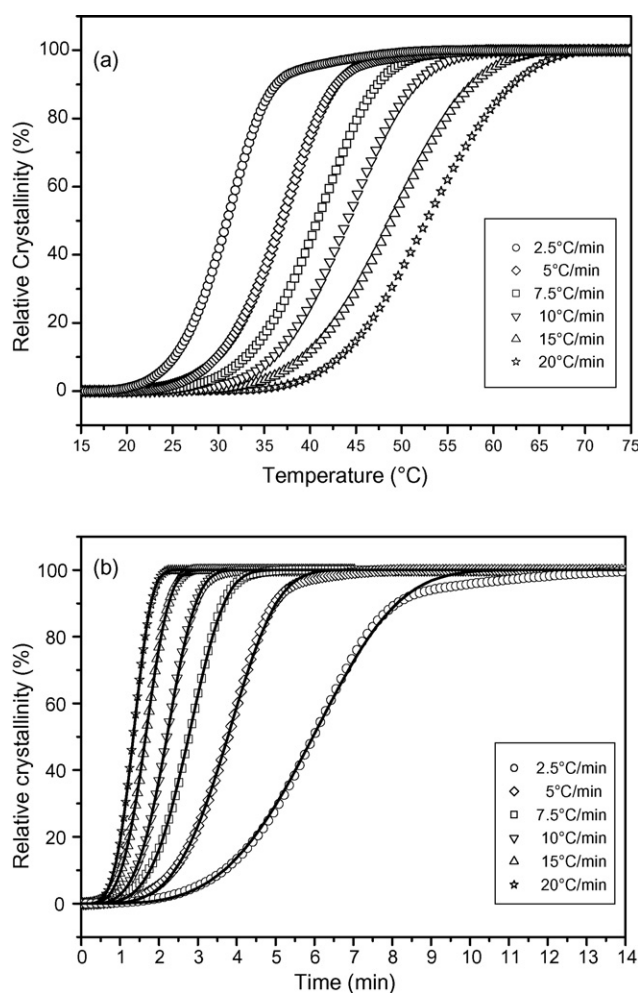


Fig. 5. Plots of relative crystallinity as a function of: (a) temperature and (b) time, during non-isothermal cold-crystallization of PESu 0.15. The geometrical points represent experimental data while the continuous line the results of the theoretical Avrami model.

The crystallization temperature T_c , can be converted to crystallization time, t , with the well-known relationship for non-isothermal crystallization processes that is strictly valid when the sample experiences the same thermal history as designed by the DSC furnace: [34]

$$t = \frac{(T_c - T_0)}{a} \quad (3)$$

where a is the constant heating rate.

The evolution of the relative crystallinity as a function of temperature for PESu 0.15 appears in Fig. 5a. $X(T)$ is converted to $X(t)$ using Eq. (3) and the data thus obtained are illustrated in Fig. 5b using geometrical points for the different heating rates used.

To quantitatively describe the evolution of the crystallinity during nonisothermal crystallization, a number of models have been proposed in the literature [14]. The most common approach is that based on a modified Avrami equation. In this investigation, the modified-Avrami, the Ozawa and the Tobin method were tested.

3.3.1. Modified Avrami method

According to the modified Avrami method, the relative degree of crystallinity, X , can be calculated from:

$$X = 1 - \exp(-Z_t t^n) \quad \text{or} \quad X = 1 - \exp[-(K_{\text{Avrami}} t)^n] \quad (4)$$

where Z_t and n denote the growth rate constant and the Avrami exponent, respectively. Since the units of Z_t are a function of n , equation (4) can be written in the composite-Avrami form using K_{Avrami} instead of Z_t (where $Z_t = K_{\text{Avrami}}^n$) [35].

Parameters Z_t and n are usually estimated by taking the logarithm of Eq. (4). In this paper, instead of this linear fitting transformation, a non-linear curve fitting procedure was employed. Accordingly, the theoretical Eq. (4) was used to fit the experimental data over the whole relative degree of crystallinity range (0–100%). The non-linear curve-fitting algorithm used was based on the Levenberg–Marquardt method (from the built-in software of Origin v7., from OriginLab Corporation) and the best fitting values for the parameters n , Z_t and K_{Avrami} are presented in Table 2. In Fig. 5b theoretical model simulation results are compared to experimental data for the PESU-0.15 sample for all heating rates examined. In all different samples and heating rates the correlation coefficient, R^2 , was greater than 0.997. It is obvious that the modified-Avrami method can describe the experimental data very well, at every heating rate used.

Since the rate of nonisothermal crystallization depends on α it has been proposed that the crystallization rate constant Z_t can be properly corrected to obtain the corresponding rate constant at unit cooling or heating rate, Z_c : [34]

$$\log Z_c = \frac{\log Z_t}{a} \quad (5)$$

The obtained Z_c values are summarized in Table 2. The values of n estimated ranged between 3.4 and 4.7 showing three-dimensional growth with thermal nucleation. Approximately the same range of variation of n (i.e. between 3.5 and 4.1) was also reported by Qiu et al. [12]. No significant trend of n with the heating rate was noticed. In contrast, the values of Z_t and Z_c were found to increase with heating rate. An explanation for this observation follows. The crystallization rates of a polymer

Table 2
Parameters obtained after the Avrami analysis for the non-isothermal cold-crystallization of PESu samples

Polymer	a ($^{\circ}\text{C}/\text{min}$)	n	Z_t (min^{-n})	K_{Avrami} (min^{-1})	Z_c
PESu 0.15	2.5	3.88	6.8×10^{-4}	0.1526	0.0541
	5.0	4.21	0.0026	0.2432	0.3041
	7.5	4.22	0.0095	0.3317	0.5375
	10	4.14	0.0263	0.4153	0.6950
	15	3.94	0.0950	0.5502	0.8548
	20	4.14	0.2057	0.6825	0.9240
PESu 0.28	2.5	4.95	7×10^{-4}	0.1447	0.0218
	5.0	4.20	0.0033	0.2567	0.3191
	7.5	4.15	0.0144	0.3602	0.5684
	10	3.65	0.0389	0.4108	0.7228
	15	4.05	0.0912	0.5536	0.8524
	20	4.34	0.1585	0.6541	0.9120
PESu 0.41	2.5	3.94	7.7×10^{-4}	0.1621	0.0568
	5.0	4.69	0.0017	0.2564	0.2793
	7.5	3.82	0.0147	0.3514	0.5699
	10	3.79	0.0627	0.4814	0.7581
	15	3.34	0.2428	0.6545	0.9099
	20	3.83	0.3860	0.7799	0.9535
PESu 0.57	2.5	3.82	8.9×10^{-4}	0.1590	0.0602
	5.0	4.28	0.0032	0.2611	0.3168
	7.5	4.24	0.0127	0.3569	0.5585
	10	3.84	0.0520	0.4630	0.7440
	15	3.52	0.2387	0.6657	0.9089
	20	3.43	0.4396	0.7869	0.9597

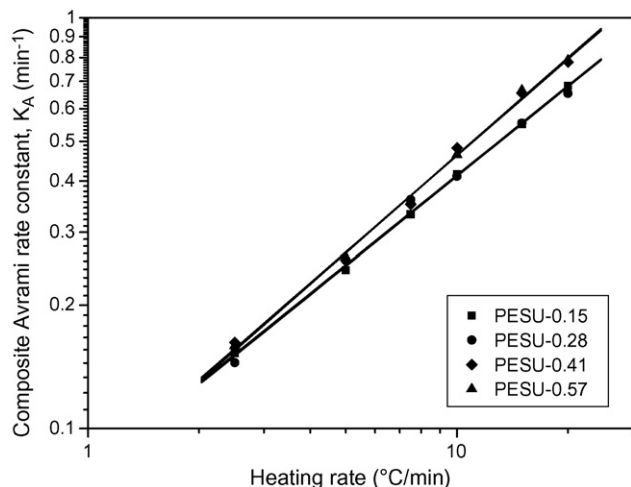


Fig. 6. Plot of the composite-Avrami rate constant as a function of the heating rate for non-isothermal cold-crystallization of all PESu samples.

show a maximum at temperatures between the glass transition temperature T_g and its melting point T_m . At low temperatures nucleation is favored while at temperatures close to T_m diffusion is faster. From a previous study on PESu, using PLM for the growth rates and DSC for the overall crystallization rates under isothermal conditions, it was concluded that faster rates are achieved in the vicinity of 55 °C [22]. Since at high heating rates cold-crystallization takes place at this temperature region, it is reasonable the Z_i and Z_c to increase with the heating rate. However, as it was reported the maximum crystallinity value achieved in such a case is lower. This occurs because the time for crystallization is limited comparing to the cases of slower heating rates as it is clearly shown in Fig. 5b. Moreover, it seems that at low heating rates the values of the Avrami rate constant are not influenced much by the different molecular weight of the samples. In contrast at high heating rates (greater than 10 °C/min) samples with higher molecular weight present also higher values of K_{Avrami} .

Concerning the values of Z_c , it was observed (Table 2) that they become constant only at high cooling rates (greater than 10 °C/min). Moreover, it was noticed that the composite-Avrami rate constant correlates very well with the heating rate in a double-logarithmic plot. Thus, by plotting $\log(K_{Avrami})$ versus $\log(\alpha)$ very good straight lines were obtained for all PESu samples (Fig. 6). The correlation equation can be expressed as:

$$\log(K_{Avrami}) = C_1 + C_2 \log(\alpha) \quad (6)$$

where C_1 and C_2 denote the intercept and the slope of the straight lines obtained, respectively.

Values of the constants C_1 and C_2 together with the correlation coefficient R^2 appear in Table 3. It was estimated that R^2 is always greater than 0.994. Therefore it seems that Eq. (6) describes well the correlation of the composite-Avrami rate constant and the heating rate in non-isothermal crystallization experiments. A similar slope (approximately equal to 0.8) was also estimated for poly(butylene succinate).

Table 3

Values of the constants C_1 and C_2 according to Eq. (6) and correlation coefficient, R^2

Sample	C_1	C_2	R^2
PESU-0.15	-1.110	0.725	0.999
PESU-0.28	-1.106	0.722	0.994
PESU-0.41	-1.116	0.780	0.995
PESU-0.57	-1.120	0.788	0.997

3.3.2. Ozawa analysis

According to the Ozawa theory the nonisothermal crystallization process is the result of an infinite number of small isothermal crystallization steps and the degree of conversion at temperature T , $X(T)$, can be calculated as: [36]

$$\ln[1 - X(T)] = -\frac{K^*(T)}{a^m} \quad (7)$$

where m is the Ozawa exponent that depends on the dimension of crystal growth and K^* is the cooling or heating crystallization function. K^* is related to the overall crystallization rate and indicates how fast crystallization occurs. Taking the double-logarithmic form of Eq. (7), it follows:

$$\log\{-\ln[1 - X(T)]\} = \log K^*(T) - m \log a \quad (8)$$

By plotting $\log\{-\ln[1 - X(T)]\}$ versus $\log a$, a straight line should be obtained and the kinetic parameters, m and K^* can be achieved from the slope and the intercept, respectively. Ozawa plots for cold-crystallization of PESu 0.15 are shown in Fig. 7. It is important to note that using values, which correspond to a degree of crystallinity in the range between 5% and 95%, the linearity in the plots is very satisfactory. It seems that the model works well for the specific polymer, maybe because of limited secondary crystallization. In other cases of polymers where extensive secondary crystallization occurs, the Ozawa model could not describe non-isothermal crystallization, but in general major problems were found for very low (less than 5%) or very high (exceeding 95%) crystallinity values, which induce curvature of the plots [13]. The calculated values for the Ozawa exponent m were found to range between 2 and 3 (Table 4). Thus, the Ozawa exponent was less than the Avrami exponent. Also the

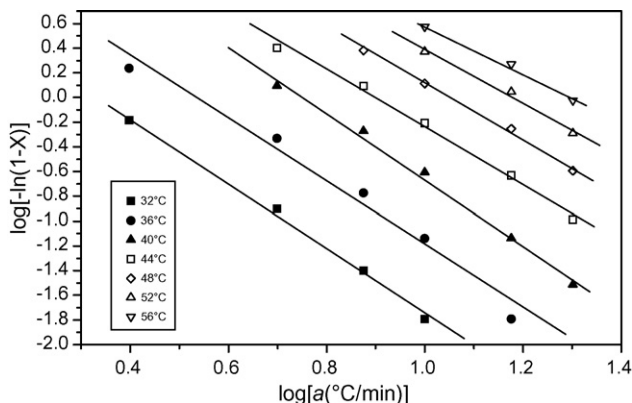


Fig. 7. Plots of $\log[-\ln(1 - X)]$ against $\log a$ for various temperatures (Ozawa plots) for non-isothermal cold-crystallization of PESu 0.57.

Table 4

Parameters obtained after the Ozawa analysis for the non-isothermal cold-crystallization of PESu samples

T (°C)	PESu 0.15		PESu 0.28		PESu 0.57	
	m	K^* ((°C/min) ^{m})	m	K^* ((°C/min) ^{m})	m	K^* ((°C/min) ^{m})
28	2.52	3.02				
32	2.48	10.00	2.97	16.60	2.65	7.94
36	2.20	17.78	2.58	31.62	2.56	23.44
40	2.20	47.86	2.89	151.36	2.71	112.20
44	2.20	102.33	2.85	323.59	2.32	120.23
48	2.15	194.98	2.47	281.84	2.26	234.42
52	1.90	186.21	2.42	512.86	2.18	371.54
56	2.06	512.86	2.16	446.68	1.96	354.81

Ozawa crystallization function $K(T)$ was found to increase rather exponentially with the crystallization temperature. This means that the crystallization rates below 56 °C increase exponentially with temperature, as would be expected. As was reported in the previous section, the maximum crystallization rates were anticipated close to 50–55 °C. This was also evidenced by the Ozawa analysis. Comparison showed that the $K(T)$ values were faster for the PESu 0.28 polymer. In general it is known for polymers that the crystallization rates increase with molecular weight for very low values due to the effect of nucleation, but decrease for high molecular weight, as the growth rates are limited because of reduced chain mobility. It seems that PESu samples show such a behavior with PESu 0.28 ($M_n = 6800$) to be the one with the faster rates among the studied samples.

3.3.3. Tobin analysis

The Avrami model is suitable for describing the early stages of crystallization. Complications arise from the effects of growth site impingement and secondary crystallization process, which were disregarded for the sake of simplicity in the original derivation of the model. Tobin proposed a theory for crystallization with growth site impingement [37–39]. According to this approach, the relative crystallinity function of time $X(t)$ can be expressed in the following form:

$$X(t) = \frac{(K_T t)^{n_T}}{1 + (K_T t)^{n_T}} \quad (9)$$

where K_T and n_T are the Tobin crystallization rate constant and the Tobin exponent, respectively. The exponent n_T need not be an integer and is governed by different types of nucleation and growth mechanisms. Eq. (9) can be rewritten in its logarithmic

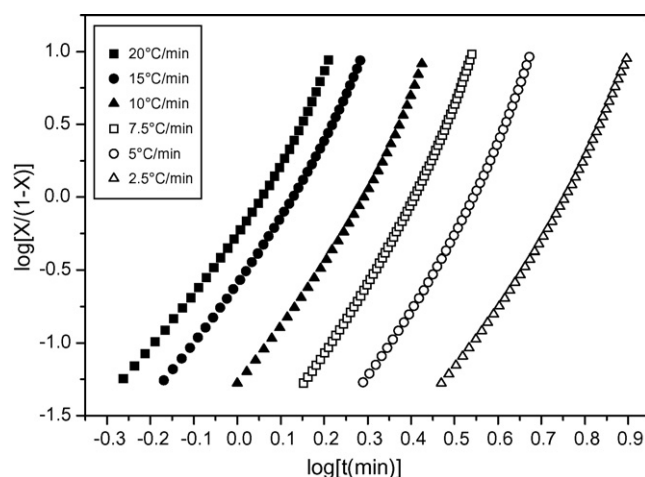


Fig. 8. Plots of $\log [X/(1 - X)]$ against $\log t$ for various heating rates (Tobin plots) for non-isothermal cold-crystallization of PESu 0.57.

form as follows:

$$\log \left[\frac{X(t)}{(1 - X(t))} \right] = n \log K_T + n_T \log t \quad (10)$$

The parameters n_T and K_T can be obtained from the slope and intercept of the plots of $\log[X(t)/(1 - X(t))]$ against $\log t$. The respective plots for PESu 0.57 are shown in Fig. 8 and the values of the calculated parameters are shown in Table 5. The Tobin exponent was always close to 5 (compared to 4 for the Avrami exponent). These values were similar to those reported by Qiu et al. [12] In the plots of Fig. 8 it is obvious that there exists a positive deviation from linearity when the degree of crystallinity is more than 50%. This proves that there is an overestimation of the spherulite impingement in the case of

Table 5

Parameters obtained after the Tobin analysis for the nonisothermal crystallization of PESu samples

a (°C/min)	PESu 0.15		PESu 0.28		PESu 0.57	
	n_T	K_T (min ⁻¹)	n_T	K_T (min ⁻¹)	n_T	K_T (min ⁻¹)
2.5	5.13	0.174	6.44	0.163	5.27	0.181
5	5.34	0.275	5.47	0.288	5.81	0.294
7.5	5.26	0.375	5.42	0.406	5.79	0.402
10	5.39	0.469	4.80	0.473	5.11	0.527
15	5.11	0.626	5.33	0.624	4.85	0.766
20	5.61	0.769	5.74	0.734	4.58	0.911

PESu. This may have to do with the small nucleation density of PESu.

3.4. Spherulite growth rates/Lauritzen–Hoffman analysis

Apart from the aforementioned macroscopic kinetic models it would be also interesting to evaluate the microscopically measured spherulite growth rate. One of the most widely accepted theories, describing the temperature dependence of the growth rate is the Lauritzen–Hoffmann theory [40]. The major application area of this theory is polymer crystallisation under isothermal conditions, while it has also been used under non-isothermal conditions [35,41]. Accordingly, the spherulite growth rate, G , is given as a function of the crystallisation temperature, T_c , by the following bi-exponential equation [40]:

$$G = G_0 \exp \left[-\frac{U^*}{R(T_c - T_\infty)} \right] \exp \left[-\frac{K_g}{T_c(\Delta T)f} \right] \quad (11)$$

where G_0 is the pre-exponential factor, and the first and second exponential terms contain the contribution of diffusion and nucleation process to the growth rate, respectively; U^* denotes the activation energy which characterizes molecular diffusion across the interfacial boundary between melt and crystals and T_∞ is the temperature below which diffusion stops; K_g is a nucleation constant and ΔT denotes the degree of undercooling ($\Delta T = T_m^0 - T_c$); f is a correction factor which is close to unity at high temperatures and is given as $f = 2T_c/(T_m^0 + T_c)$; the equilibrium melting temperature, T_m^0 can be calculated using some extrapolative procedure like the linear or nonlinear Hoffman–Weeks extrapolation.

The nucleation parameter, K_g , can be calculated from Eq. (11) using the double logarithmic transformation:

$$\ln(G) + \frac{U^*}{R(T_c - T_\infty)} = \ln(G_0) - \frac{K_g}{T_c(\Delta T)f} \quad (12)$$

Plotting the left-hand side of Eq. (12) with respect to $1/(T_c(\Delta T)f)$ a straight line should appear having a slope equal to K_g . Critical break points, identified by the change in the slope of the line, when appear in such a plot, have been attributed to regime transitions accompanied by morphological changes of the crystals formed (i.e. change from axialite-like to banded spherulite and non-banded spherulite morphology).

Subsequently Eq. (12) was used to determine the effect of the molecular weight of the PESu samples on the nucleation constant K_g . Values for the glass transition and equilibrium melting temperatures were taken from [22], i.e. $T_m^0 = 114^\circ\text{C}$ and $T_g = -11.5^\circ\text{C}$ (T_m^0 was estimated using a linear Hoffman–Weeks extrapolation while T_g was measured using DSC). Furthermore, it was reported there that using the WLF values ($U^* = 4200$ cal/mol and $T_\infty = T_g - 51.6$ K), for the PESu 0.28 sample, regime II to regime III transition is observable at approximately 70°C [22], in agreement with findings by Gan et al. [10]. The ratio of K_g^{III}/K_g^{II} was 1.8, close to the expected value 2.0 according to the secondary nucleation theory. It will be shown later in the paper that using the value of 4200 cal/mol for U^* is a good approximation if a fixed value for this parameter should

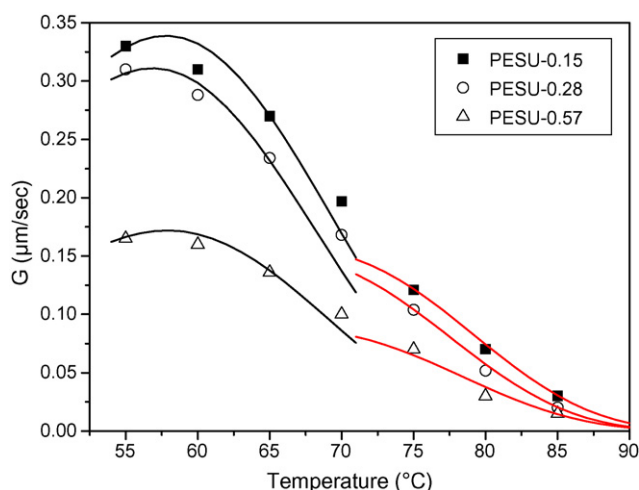


Fig. 9. Spherulite growth rate as a function of crystallization temperature for melt crystallization of PESu samples with different molecular weight obtained from isothermal PLM measurements. Solid lines are fits to the Lauritzen–Hoffman theory according to Eq. (11).

be used. The spherulite growth rates, G , for the three PESu samples 0.15, 0.28 and 0.57, was measured during crystallization from the melt under isothermal conditions at various temperatures in the range from 55 to 85°C using PLM. Fig. 9 shows the dependence of the spherulite growth rates on crystallization temperature for the three samples. It is obvious that the rates decrease with increasing molecular weight in this temperature range. The experimental data were further analysed using the previously reported parameters according to the Lauritzen–Hoffman theory. The respective plots can be seen in Fig. 10. It was found that a regime transition takes place for all the samples in the vicinity of 70°C and the K_g^{III}/K_g^{II} ratio was about 1.7–1.8. For the lower temperature region (below 70°C) and from the slope of the linear curves, the K_g^{III} values were estimated to be equal to 1.87×10^5 , 1.90×10^5 and 1.91×10^5 K^2 for PESu-0.15, PESu-0.28 and PESu-0.57, respectively. The estimated results do not show any clear effect of the samples' average molecular weight on the value of the nucleation constant K_g . Once the values of K_g

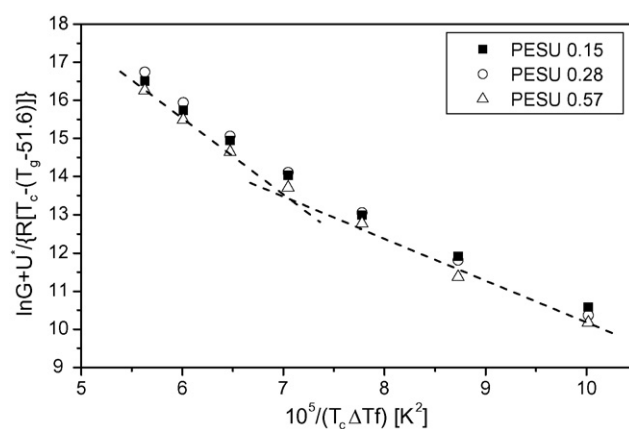


Fig. 10. Lauritzen–Hoffman type plots constructed from spherulite growth rate data obtained from isothermal PLM experiments for the PESu samples with different molecular weight.

were determined, the growth rate, G , can be theoretically predicted from Eq. (11). Results are plotted in Fig. 9 and compared to the experimental data, since according to Müller et al. [42] use of a linear scale highlights the differences between experiment and theory which are masked in Fig. 10 by the use of logarithms and reduced parameters. Two theoretical curves with different K_g values are plotted for every PESu sample, since a regime transition was noticed around 70 °C. It can be seen that the estimated K_g values when employed in Eq. (11) result to a rather good fitting of the experimental data by the theoretical equation.

Instead of using PLM measurements, several authors have treated the isothermal crystallisation rate data obtained by DSC, according to the Lauritzen–Hoffmann analysis (Eq. (12)) and assumed that G is proportional to the inverse of the crystallisation half time ($G \approx 1/t_{1/2}$) [43–45]. The validity of such an attempt has been tested in [46]. Furthermore, during non-isothermal crystallization a modified Lauritzen–Hoffman model can be used by substituting T_c with $T_o + at$, where T_o denotes the onset temperature of the cold-crystallization. The resulting equation is as follows:

$$\ln G + \frac{U^*}{R(T_o + at - T_\infty)} = \ln G_o - \frac{K_g}{(T_o + at)[T_m^o - (T_o + at)]f} \quad (13)$$

Eq. (13) was used in this study in order to estimate the K_g using non-isothermal cold-crystallization data of different PESu samples obtained from DSC. The above mentioned assumption was used for the growth rate, i.e. $G \approx 1/t_{1/2}$. Thus, the crystallization temperature and time at 50% degree of crystallinity were used (i.e. $t = t_{1/2}$). These Lauritzen–Hoffman type plots for different PESu samples appear in Fig. 11a. Since the temperature range of the measurements was always below 70 °C, crystallization regime III was assumed. The obtained values for K_g^{III} were found to be equal to 2.48×10^5 , 2.62×10^5 , 2.47×10^5 and 2.45×10^5 K² for the PESu-0.15, PESu-0.28, PESu-0.41 and PESu-0.57 polymers, respectively. The regression coefficient R^2 was in the vicinity of 0.98. These values are comparable to those reported previously, though slightly higher. However, they were obtained from a totally different experimental method, meaning that in this case the data were collected from non-isothermal cold-crystallization DSC experiments instead of isothermal from PLM. In addition, these data were calculated at a lower range of crystallization temperatures (from 30 to 56 °C) compared to corresponding from PLM measurements (55 to 70 °C). Again, the effect of the samples' average molecular weight on K_g was not clear. Moreover, in order to have more comparable results, the nucleation constant K_g was estimated once again but using experimental data from [22] from isothermal DSC measurements and the assumption, $G \approx 1/t_{1/2}$. Comparable Lauritzen–Hoffman type plots for PESu-0.28 obtained from isothermal and non-isothermal DSC measurements together with isothermal PLM measurements appear in Fig. 11b. The K_g estimated in the temperature region 50–70 °C (the same as that used in isothermal PLM measurements) was 2.44×10^5 K², again a value higher than that

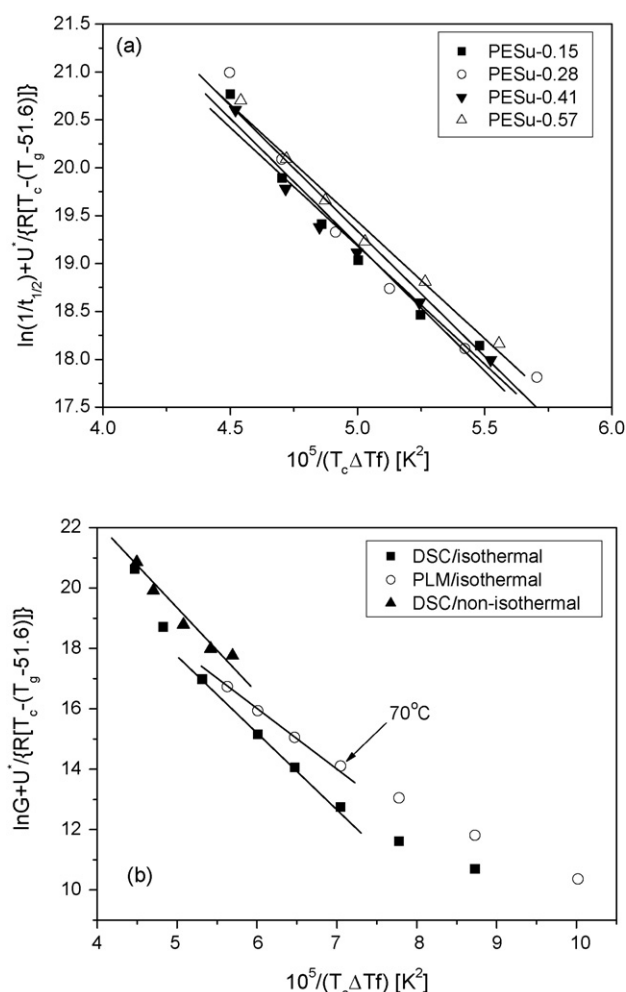


Fig. 11. Lauritzen–Hoffman type plots constructed from (a) DSC non-isothermal rate data for the PESu samples, using the inverse of the half crystallization time in place of G and (b) DSC isothermal and non-isothermal and PLM isothermal data for the PESu-0.28 sample.

estimated from isothermal PLM measurement and close, though slightly lower, than that calculated from non-isothermal DSC measurements. A good explanation on this result is given by Müller et al. [42]. Accordingly, the values obtained from DSC measurements deal with overall crystallization rates including both nucleation and growth, while those estimated from PLM measurements are growth only dependent. Therefore, it seems that the process of nucleation and growth has a larger energetic barrier than the process of spherulite growth only. The increase in the estimation of K_g is almost 28%, approximately the same with that reported in [42].

Moreover, it was examined if a better estimation of the K_g values (i.e. resembling those measured from PLM) could be obtained if a different characteristic time will be used in place of G . Therefore, the growth rate was assumed equal to the inverse of the crystallization time to achieve 2% relative degree of crystallinity ($G = 1/t_{0.02}$). Although a good linear dependence was found in all cases, the values of K_g calculated ranged between 4 and 5×10^5 K² much higher than those from PLM measurements. This can be attributed to a much lower temperature range

involved in these measurements (i.e. from 20 to 40 °C) together with uncertainties in the calculation of the crystallization rate at 2% relative degree of crystallinity.

3.5. Estimation of the Lauritzen–Hoffman parameters (U^* and K_g) using the Vyazovkin–Sbirrazzuoli method

Since the values of K_g estimated from the Lauritzen–Hoffman analysis did not show any clear effect of the sample average molecular weight, they were further estimated in this section using an isoconversional approach and the overall rates of nonisothermal crystallization, according to the method of Vyazovkin and Sbirrazzuoli [23]. To this direction initially the effective activation energy as a function of relative crystallinity should be estimated using an isoconversional approach. The use of multiple heating rate methods such as isoconversional methods is quite helpful and recommended in detecting and elucidating complex kinetics in polymeric systems [47]. Among the isoconversional approaches, the differential method of Friedman [48] and the advanced integral method of Vyazovkin and Sbirrazzuoli [49] are the most appropriate [50]. In this investigation the method of Friedman was used. According to the differential isoconversional method of Friedman, different effective activation energies are calculated for every degree of crystallinity from

$$\ln \left(\frac{dX}{dt} \right)_{X,i} = \text{Const} - \frac{\Delta E_X}{RT_{X,i}} \quad (14)$$

where dX/dt is the instantaneous crystallization rate as a function of time at a given conversion X , ΔE_X is the effective activation energy at a given conversion X , $T_{X,i}$ is the set of temperatures related to a given conversion X at different heating rates a_i , and the subscript i refer to every individual heating rate used.

According to this method, the $X(t)$ function obtained from the integration of the experimentally measured crystallization rates is initially differentiated with respect to time to obtain the instantaneous crystallization rate, dX/dt . Furthermore, by selecting appropriate degrees of crystallinity (i.e. from 2% to 98%) the values of dX/dt at a specific X are correlated to the corresponding crystallization temperature at this X , i.e. T_X . Then by plotting the left hand side of Eq. (14) with respect to $1/T_X$ a straight line must be obtained with a slope equal to $\Delta E_X/R$. Indicative plots appear in Fig. 12. Almost linear curves were obtained at relative degrees of crystallinity less than approximately 70%, whereas at higher X a curvature in the plots was obvious. This means that the results on ΔE_X calculated at high values of X are not reliable.

The effective activation energy, thus obtained was subsequently plotted as a function of the relative degree of crystallinity as one can see in Fig. 13. Since different heating rates are involved during the cold-crystallization experiments, positive values for ΔE_X were estimated in contrast to melt-crystallization, where negative values are usually estimated. From Fig. 13 it can be seen that the effective activation energy decreases with conversion for the cold-crystallization. This decrease is expected from the theoretical dependence of ΔE versus T , keeping in mind that X increases with temperature [51].

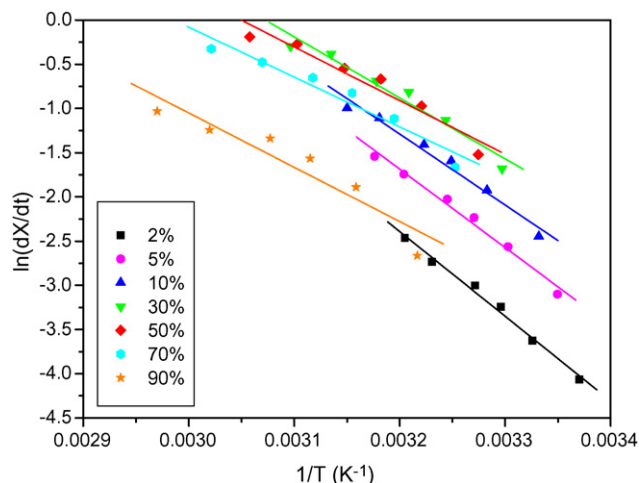


Fig. 12. Plot of $\ln(dX/dt)$ vs. $1/T$ for the PESu-0.57 non-isothermal cold-crystallization at different heating rates and relative degrees of crystallinity from 2% to 90%.

The values for the polymer with the higher molecular weight were slightly higher compared to samples with lower average molecular weight. This may be related to slower nucleation of PESu 0.15. In contrast the PESu 0.57 has a very higher molecular weight and the increased value of ΔE is probably associated to decreased diffusion rates. In order to test this hypothesis, a plot of ΔE versus T was constructed by replacing X with an average T , according to the method proposed by Vyazovkin and Sbirrazzuoli [47]. This plot for different PESu samples appears in Fig. 14. The values of ΔE decrease with temperature until 46 °C (corresponding to 70% degree of crystallinity), whereas afterwards they tend to increase.

According to Vyazovkin and Sbirrazzuoli [23,47], the most attractive feature in applying the isoconversional methods to DSC data is that the resulting ΔE_X dependencies can be utilized for estimating the parameters of the Lauritzen–Hoffman theory. Eq. (11) has been used to derive the temperature dependence

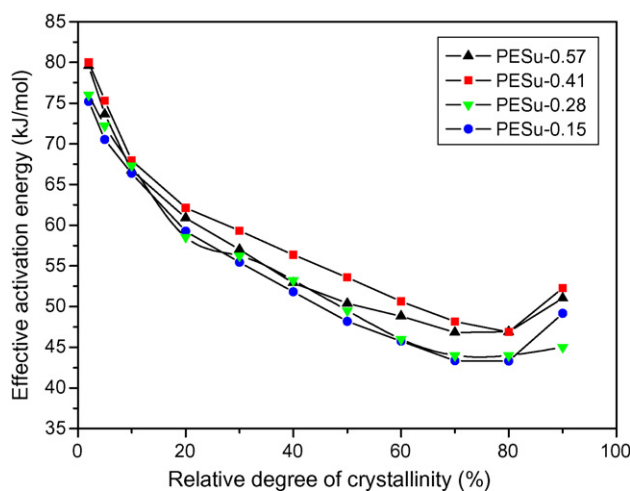


Fig. 13. Dependence of the effective activation energy on the relative degree of crystallinity (isoconversional analysis) for the PESu samples obtained using the differential method of Friedman.

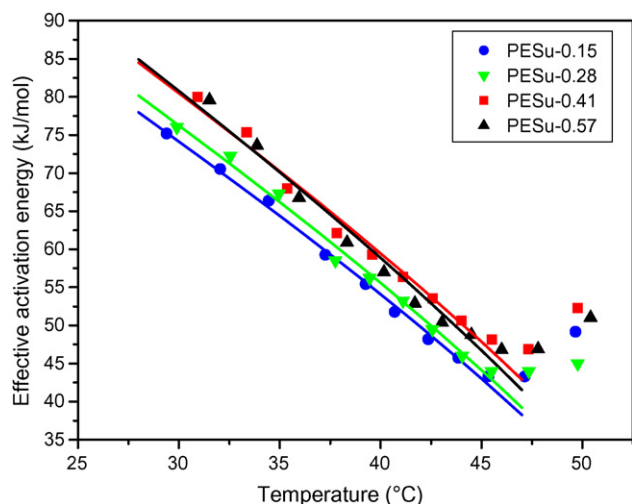


Fig. 14. Effective activation energy as a function of temperature calculated using the method of Friedman for different PESu samples (geometrical points). The continuous lines represent the best fit to the experimental data using Eq. (15) and $X < 70\%$.

of the effective activation energy of the growth rate as follows [23]:

$$\begin{aligned} \Delta E &= -R \frac{d(\ln G)}{d(1/T)} \\ &= U^* \frac{T^2}{(T - T_\infty)^2} + K_g R \frac{(T_m^0)^2 - T^2 - T_m^0 T}{(T_m^0 - T)^2 T} \end{aligned} \quad (15)$$

Thus the temperature dependence of the effective activation energy derived from DSC data (e.g. from the method of Friedman) can be fit to Eq. (15) to evaluate the Lauritzen–Hoffman parameters K_g and U^* for all different molecular weight samples. It should be noted that in the estimation procedure only data points corresponding to $X < 70\%$ were employed, since the plots used to estimate ΔE at $X > 70\%$ showed a curvature. The Levenberg–Marquardt method was used as a non-linear fitting algorithm (from the built-in software of Origin v7., from Origin-Lab Corporation). The best fit values for K_g and U^* appear in Table 6. The numerical values of K_g appear to range in between the corresponding calculated from isothermal PLM measurements and non-isothermal DSC using the approximation $G = 1/t_{1/2}$, though closer to those obtained from PLM data. Again a clear dependence of K_g on the sample average molecular weight was not observed. However, a very interesting result came from the estimated values of U^* . The first point is that

the best fit values for U^* are close to the constant value of 4200 cal/mol used in the isothermal crystallization experiments. Verifying thus the initial assumption made. Furthermore, a clear increase of U^* with the polymer average molecular weight was obtained. Since U^* is an activation energy which characterizes molecular diffusion across the interfacial boundary between melt and crystals, it seems that the effect of diffusion is more pronounced in polymers having higher average molecular weight.

Finally, better results should have been obtained if both melt and glass crystallization data were used, according to a recent publication carried out for PET and PEN [51]. However, this is not possible for PESu samples since it experiences very slow crystallization rates from the melt.

4. Conclusions

The cold-crystallization of PESu was found to be affected by the molecular weight of the polymer, meaning that an increase in the cold-crystallization temperature was in general found with increasing molecular weight. Also the ultimate degree of crystallinity decreased with molecular weight. Recrystallization takes place before melting of the cold-crystallized samples. The Step Scan DSC showed that the multiple melting behavior observed in standard DSC traces is the result of two recrystallization exotherms and two melting peaks. The recrystallization is more significant for low molecular weight PESu. The kinetics of cold-crystallization was analyzed using several models. The Avrami and Ozawa models were found to give satisfactory results in contrast to the Tobin model. The nucleation constant K_g of the Lauritzen–Hoffmann equation was estimated using either isothermal PLM measurements or non-isothermal DSC cold-crystallization data and the assumption $G = 1/t_{1/2}$. No clear trend of K_g with the polymer molecular weight was observed. Finally, both Lauritzen–Hoffman parameters were evaluated using an isoconversional analysis and the overall rates of non-isothermal cold-crystallization. A clear increase of U^* with the molecular weight was observed meaning that polymers with longer chains are influenced more by diffusional phenomena.

Acknowledgements

This work was funded by the Greek Ministry of Education (EPEAEK Pythagoras I, 89206, RC AUTH 21914). DSA would like also to thank Prof. A. Müller for sending a reprint of reference 42.

References

- [1] D. Bikiaris, J. Aburto, I. Alric, E. Borredon, M. Botev, C. Betchev, C. Panayiotou, J. Appl. Polym. Sci. 71 (1999) 1089.
- [2] J. Aburto, I. Alric, S. Thiebaud, E. Borredon, D. Bikiaris, J. Prinos, C. Panayiotou, J. Appl. Polym. Sci. 74 (1999) 1440.
- [3] R.D. Fields, F. Rodriguez, R.K. Finn, J. Appl. Polym. Sci. 18 (1974) 3571.
- [4] G. Montaudo, P. Rizzarelli, Polym. Degrad. Stab. 70 (2000) 305.
- [5] D.K. Song, Y.K. Sung, J. Appl. Polym. Sci. 56 (1995) 1381.
- [6] G. Seretoudi, D. Bikiaris, C. Panayiotou, Polymer 43 (2002) 5405.
- [7] W. Shen-Guo, Q. Bo, Polym. Adv. Techn. 4 (1992) 363.

Table 6

Values of the Lauritzen–Hoffman parameters, K_g and U^* evaluated using an isoconversional approach and the overall rates of non-isothermal cold-crystallization for different PESu samples

Sample	K_g (K^2)	U^* (cal/mol)	R^2
PESU-0.15	2.1×10^5	4132	0.996
PESU-0.28	2.17×10^5	4255	0.993
PESU-0.41	2.17×10^5	4429	0.984
PESU-0.57	2.3×10^5	4508	0.986

- [8] K. Chrissafis, K.M. Paraskevopoulos, D.N. Bikiaris, *Thermochim. Acta* 435 (2005) 142.
- [9] Y. Ichikawa, K. Nogushi, K. Okuyama, J. Washiyama, *Polymer* 42 (2001) 3703.
- [10] Z. Gan, H. Abe, Y. Doi, *Biomacromolecules* 1 (2000) 704.
- [11] R. Caminiti, A. Isopo, M.A. Orru, V.R. Albertini, *Chem. Mater.* 12 (2000) 369.
- [12] Z. Qiu, T. Ikehara, T. Nishi, *Polymer* 44 (2003) 5429.
- [13] Z. Qiu, S. Fujinami, M. Komura, K. Nakajima, T. Ikehara, T. Nishi, *Polymer* 45 (2004) 4515.
- [14] M.L. Di Lorenzo, C. Silvestre, *Prog. Polym. Sci.* 24 (1999) 917.
- [15] M.J. Avrami, *J. Chem. Phys.* 7 (1939) 1103.
- [16] M.J. Avrami, *J. Chem. Phys.* 8 (1940) 812.
- [17] M.J. Avrami, *J. Chem. Phys.* 9 (1941) 177.
- [18] N. Kolmogorov, *Izv. Akad. Nauk. SSSR* 3 (1937) 355.
- [19] A. Johnson, R.F. Mehl, *Trans. Am. Inst. Mining Metall. Eng.* 135 (1939) 416.
- [20] D.N. Bikiaris, G.Z. Papageorgiou, S.D. Achilias, *Polym. Degrad. Stab.* 91 (2006) 31.
- [21] D.N. Bikiaris, D.S. Achilias, *Polymer* 47 (2006) 4851.
- [22] G.Z. Papageorgiou, D.N. Bikiaris, *Polymer* 46 (2005) 12081.
- [23] S. Vyazovkin, N. Sbirrazzuoli, *Macromol. Rapid Commun.* 25 (2004) 733.
- [24] C.P. Roupakias, D.N. Bikiaris, G.P. Karayannidis, *J. Polym. Sci. Part A, Polym. Chem.* 43 (2005) 3988.
- [25] K. Chrissafis, K.M. Paraskevopoulos, D.N. Bikiaris, *Thermochim. Acta* 440 (2006) 166.
- [26] O.F. Solomon, I.Z. Ciuta, *J. Appl. Polym. Sci.* 6 (1962) 683.
- [27] B. Wunderlich, *Prog. Polym. Sci.* 28 (2003) 383.
- [28] B.B. Sauer, W.G. Kampert, E. Neal Blanchard, S.A. Threefoot, B.S. Hsiao, *Polymer* 41 (2000) 1099.
- [29] G.Z. Papageorgiou, G.P. Karayannidis, *Polymer* 40 (1999) 5325.
- [30] M.-Y. Ju, F.-C. Chang, *Polymer* 42 (2001) 5037.
- [31] Z.G. Wang, X.H. Wang, B.S. Hsiao, R.A. Philips, F.J. Medellin-Rodriguez, S. Srinivas, H. Wang, C.C. Han, *J. Polym. Sci., Part B: Polym. Phys.* 39 (2001) 2982.
- [32] Y.S. Sun, E.M. Woo, *Macromolecules* 32 (1999) 7836.
- [33] H. Marand, A. Alizadeh, R. Farmer, R. Desai, V. Velikov, *Macromolecules* 33 (2000) 3392.
- [34] A. Jeziorny, *Polymer* 19 (1978) 1142.
- [35] D.S. Achilias, G.Z. Papageorgiou, G.P. Karayannidis, *J. Polym. Sci., Part B: Polym. Phys.* 42 (2004) 3775.
- [36] T. Ozawa, *Polymer* 12 (1971) 150.
- [37] M.C. Tobin, *J. Polym. Sci., Part B: Polym. Phys.* 12 (1974) 399.
- [38] M.C. Tobin, *J. Polym. Sci., Part B: Polym. Phys.* 14 (1976) 2253.
- [39] M.C. Tobin, *J. Polym. Sci., Part B: Polym. Phys.* 15 (1977) 2268.
- [40] J.D. Hoffman, G.T. Davis, J.I. Lauritzen, in: N.B. Hannay (Ed.), *Treatise on Solid State Chemistry*, Plenum, New York, 1976, p. 3.
- [41] B.A. Lim, K.S. McGuire, D.R. Lloyd, *Polym. Eng. Sci.* 33 (1993) 537.
- [42] A.J. Müller, J. Albuerne, L. Marquez, J.-M. Raquez, P. Degée, P. Dubois, J. Hobbs, I.W. Hamley, *Faraday Discuss.* 128 (2005) 231.
- [43] T.W. Chan, A.I. Isayev, *Polym. Eng. Sci.* 34 (1994) 461.
- [44] N. Dangseeyun, P. Shrimoan, P. Supaphol, M. Nithitanakul, *Thermochim. Acta* 409 (2004) 63.
- [45] G.Z. Papageorgiou, D.S. Achilias, D.N. Bikiaris, G.P. Karayannidis, *Thermochim. Acta* 427 (2005) 117.
- [46] D.S. Achilias, G.Z. Papageorgiou, G.P. Karayannidis, *J. Therm. Anal. Calorim.* 86 (2006) 791.
- [47] S. Vyazovkin, N. Sbirrazzuoli, *Macromol. Rapid Commun.* 27 (2006) 1515.
- [48] H.J. Friedman, *J. Polym. Sci., Part C: Polym. Symp.*, 12 (1964–1965) 405.
- [49] S. Vyazovkin, N. Sbirrazzuoli, *J. Phys. Chem. B* 107 (2003) 882.
- [50] S. Vyazovkin, *Macromol. Rapid Commun.* 23 (2002) 771.
- [51] S. Vyazovkin, I. Dranca, *Macromol. Chem. Phys.* 207 (2006) 20.